Thermochimica Acta 538 (2012) 67–74

Contents lists available at SciVerse ScienceDirect

Thermochimica Acta

journal homepage: www.elsevier.com/locate/tca

Advantageous use of SSA technique to observe effects of thickness, antioxidant and oxygen in gamma irradiated low density polyethylene

C.J. Pérez [a,*], M.D. Failla [b], J.M. Carella [a]

[a] Research Institute of Material Science and Technology (INTEMA), National Research Council (CONICET), Engineering Faculty, Mar del Plata University, Av. J.B. Justo 4302, 7600 Mar del Plata, Argentina
[b] Planta Piloto de Ingeniería Química-PLAPIQUI (UNS-CONICET), Camino "La Carrindanga" Km 7, 8000 Bahía Blanca, Argentina

ARTICLE INFO

Article history:
Received 13 December 2011
Received in revised form 14 February 2012
Accepted 22 March 2012
Available online 30 March 2012

Keywords:
Low density polyethylene
Radiation
Thermal analysis
Successive self-nucleation and annealing

ABSTRACT

Information obtained from successive self-nucleation and annealing (SSA) technique is analyzed, paying special attention to the observable effects of samples thickness and antioxidant and oxygen concentrations. Molecular structure changes for low density polyethylene (LDPE) samples, irradiated under three different atmospheres for doses between 33 and 222 kGy were analyzed, with emphasis on the changes of longer polymethylene crystallizable lengths. Antioxidant and oxygen concentrations were varied for samples of different thickness to study the effects on degradation. The changes in the molecular structure were followed simultaneously by SSA and Infrared spectroscopy (FTIR) via carbonyl group concentration. Preliminary quantifications of the SSA technique sensitivity are also advanced.

1. Introduction

The properties of many semicrystalline polymers are routinely modified by molecular structural changes induced by free radicals, generated by peroxides decomposition or other processes like high energy radiation or electron beams. In situ formed free radicals produce on the main chain atoms a variety of reactions that end at modifying the molecular macrostructure. Polyolefins can be modified in the solid or the melt states, depending on the specific purpose of the molecular changes to be conducted. For instance, heat-shrinkable film can be made by irradiation in the solid state to produce light crosslinking that concentrate mainly in amorphous regions. To increase melt extensional viscosity for films and foams production, low-level, evenly distributed long-chain branching can be induced in some polypropylenes by irradiation in the melt state [1–3].

Free radicals generated by irradiation processes are at first homogeneously distributed, regardless of the physical state of the polymer – either liquid or semicrystalline – but the reactions paths following this initial step depend strongly on the media mobility. Free radicals located at the high-mobility amorphous regions will react relatively fast, mainly by reaction with other radicals, with antioxidants, with oxygen or with other macromolecules. Some free radicals are located in the crystalline phase, and react at a much slower rate [4,5]. Reactions of free radicals with macromolecules main chain atoms may produce chain crosslinking or scissions, depending mainly on whether the reacted carbon is a secondary or a tertiary one; secondary carbons produce much more crosslinking than tertiary ones. Reactions in the melt state produce more homogeneous molecular structural changes. Reactions in the solid state will produce in some cases – like medium and low-density polyethylene – most changes for the sectors of the molecules located in the amorphous regions that include more branched material than the average. Any characterization method that may help to distinguish between reactions of branched and linear parts of a molecule will be very useful.

Polyethylene molecular changes produced by free radicals have been widely studied by several experimental methods [6,7]. Size Exclusion Chromatography (SEC) has been used to study changes in molecular weight distributions associated with the scission and crosslinking processes. Only soluble polymer can be analyzed by SEC, excluding the gel fraction, thus limiting the usefulness to modifications of the sol fraction of the reacted polymer. Furthermore, the technique is based on fractionation by hydrodynamic volumes that can be well calculated only for polymers with a precisely controlled macrostructure. As the hydrodynamic volume for equal molecular weights is reduced by long-chain branching, the technique can be used for quantitative measurements only for model polymers with a starting narrow molecular weight distribution [8,9]. Most reliable results have been obtained for low reactions advances, because of the simultaneous scission and crosslinking processes that

* Corresponding author. Tel.: +54 223 4816600.
E-mail address: cjperez@fi.mdp.edu.ar (C.J. Pérez).

0040-6031/$ – see front matter © 2012 Elsevier B.V. All rights reserved.
http://dx.doi.org/10.1016/j.tca.2012.03.020

produce either molecular weights reductions or random branching with molecular weights increase. Another drawback comes from the simultaneous changes produced in the radius of gyration by chains scission and crosslinking that give similar values for very different molecular weights. Ultimately, the technique provides information only for changes in the large molecular scale, in the order of the radius of gyration size. Molecular changes produced for most commercial polymers at low reaction advances cannot be quantified.

SEC techniques have been assisted by solvents extraction procedures, as these can isolate the soluble fraction after the gel point has been reached. Again, best results are obtained only for model polymers with narrow molecular weight distributions and high molecular weight averages.

To study molecular changes for low reactions advances, more information is needed concerning changes occurred for smaller molecular scales, in the order of a hundred main chain carbon atoms. Some techniques could be used to detect changes in the average crystallizable lengths of polyolefin molecules. Temperature Rising Fractionation (TREF) and Crystallization Analysis Fractionation (CRYSTAF) are based on the solution equilibrium temperature for semicrystalline polymers that are slowly crystallized from diluted solutions on a large area. Fractions with larger average crystallizable sequences lengths will crystallize at higher temperatures. Semicrystalline polymer fractions with increasing average crystallizable sequences lengths can be separated by rising the solvent temperature used to solubilize the desired fractions [10–13]. The separation process–based on solid-solution thermodynamic equilibrium – has been modeled and shown to depend on temperature, polymer–solvent interaction parameter, solvent concentration that includes solvated polymer molecules, and average crystallizable sequences lengths for the whole molecule. This suggests that small changes in the crystallizable sequences lengths distributions will be very difficult to detect, as their effect on the molecule solubility will be diluted in the average for the whole molecule.

The SSA technique can give direct information on the distribution of melting temperatures for the lamellae population formed in semicrystalline homopolymers and copolymers [14,15]. Starting from the melt, the polymer samples are allowed to crystallize at selected annealing temperature values. The crystalline lamellae population thus obtained shows a discrete distribution of melting temperatures located just above the annealing temperatures [16–19]. These melting temperatures can be related to lamellae thicknesses distributions with the well-known Gibbs-Thompson equation, that has been modified to account for changes in the lamellar surface free energy associated with the increasing amount of surface defects that show up in copolymers [20–22].

The SSA technique can be considered as a selective fractionation of crystallizable lengths of polymethylene sequences lengths, because the annealing steps allow time for diffusion and growth of lamellae to an equilibrium value. Being the thicker lamellae formed first, we can imagine that the diffusion processes that contribute to forming thinner lamellae will be increasingly restricted as the crystallization temperatures are reduced, and therefore most useful information will be obtained from changes in the thicker lamellae populations. Thicker lamellae, which form at the highest annealing temperature, will reflect more faithfully the changes in molecular structure; thinner lamellae may not reach an equilibrium state, and some structural changes may be masked because of this fact [18,19].

The SSA can be performed with a conventional DSC, can be used to detect small changes in the semicrystalline structure of either the soluble or the gel fractions, and even more information can be obtained with the aid of separation techniques. Also, very small amounts of samples are enough to perform an SSA analysis [23]. We have found that small molecular structure changes produced by chains scission in the order of one carbon atom per molecule can be detected [24,25].

This work shows the usefulness of the SSA technique to detect differences in changes in polyolefins molecular structure by irradiation in different atmospheres that modify the speed ratio for crosslinking and chain scission High energy irradiation promotes the simultaneous crosslinking and scission of chains, and the relative efficiency of each one is closely related to the presence of oxygen and antioxidants. Simultaneous crosslinking and scission will produce changes in the distribution of polymethylene crystallizable sequences lengths. Crosslinking will interrupt the sequences lengths involved, while scission will also free molecular ends produced in the process [19,26]. For strictly linear chains, the effect of crosslinking or scission may be to reduce the average value for the crystallizable sequences lengths distribution, and the combined mixed effects of both reactions may be difficult to separate and analyze. For very long linear chains, chain scission might also cause crystallinity to be increased because of topological constraints reduction. Nevertheless, there is an extra detail linked to long-chain branching; as shown in earlier work. Scission of tertiary carbon atoms at the origin of long branches may cause longer crystallizable sequences lengths to free from topological constraints and incorporate to thicker lamellae during the SSA annealing stage. This process has been shown to increase thicker lamellae population [18,19].

As a test for the SSA method, we use here the technique to distinguish different effects of γ-irradiation on LDPE. LDPE samples were irradiated in contact with atmospheres with three different contents of oxygen, with and without antioxidants, and two different thickness values. Oxygen and antioxidants reduce crosslinking efficiency by reacting with free radicals, and therefore the changes on the distributions of crystallizable sequences lengths could be modified by the oxygen concentration and the presence of antioxidants.

LDPE is produced by ethylene homopolymerization in high-pressure reactors, initiated by free radicals. The polymerization process produces tertiary carbon atoms – about 1–2 mole% – and some of these are placed at the root of a small quantity of long-chain branches. This small fraction of tertiary carbon atoms is rather difficult to detect with conventional spectroscopic methods, and main effects have been observed via rheological properties [27]. Changes in the population of tertiary carbon atoms in LDPE in early stages of irradiation processes can be detected as changes in the amount of the longer crystallizable polymethylene sequences [24,25]. Here we also advance some SSA data and analysis that lead to modeling early stages of the combined scission-crosslinking process.

2. Experimental procedure

2.1. Material and sample preparation

Low Density Polyethylene (LDPE (203M)) supplied by Dow-PBB Polisur (Bahía Blanca, Argentina) was used throughout this study.

Four different types of samples were prepared by compression molding at 150 °C. Thin samples thickness is about 0.2–0.3 mm, and thick samples thickness us about 0.7–0.8 mm. Samples were prepared with and without the antioxidant content provided by manufacturer.

To strip the antioxidant, about 200 gr. of polymer were dissolved in boiling xylene, and quickly precipitated in stirred cold methanol to obtain a fine powder. Most of the antioxidant and other additives are expected to remain in the thus formed xylene–methanol solution. The precipitated polymers were exhaustively dried at room temperature.

The films were inserted into tightly capped Pyrex flasks. The total film in each flask was set in order to get equivalent total mass. Flasks were placed in a gloves box and kept under constant atmosphere for 2 days. Before closing the flasks, the gloves box was kept filled with mixtures of nitrogen/oxygen to give oxygen concentrations of 0, 21 and 100% v/v at a total pressure of 1 atm at room temperature. Subsequently these samples were exposed at room temperature to γ-rays generated by a ^{60}Co source. The dose rate was 8 kGy/h determined by dosimetry with a radiochromic thin-film dosimeter. Equal doses between 33 and 222 kGy were applied to the samples. The error in dose can be estimated in 5%.

2.2. Evaluation of basic thermal behavior

Samples were used as received (no gel extraction) throughout all DSC and SSA characterization. Small disc samples (approximately 10 mg) were cut from films of all unmodified and irradiated LDPE. The samples were encapsulated in DSC aluminum pans and ultra high purity dry nitrogen was used as an inert atmosphere for conditioning and testing in a Perkin Elmer Pyris II calorimeter. A first characterization of the thermal behavior of the polymers was performed on the DSC by cooling and heating runs between 25 and 200 °C at a heating rate of 10 °C/min. In order to erase all previous thermal history all the samples were previously held in the molten state at 150 °C for 5 min.

2.3. Successive self-nucleation and annealing (SSA)

The SSA technique consists of successive heating and cooling cycles. The self-nucleation and annealing temperatures (T_s) were chosen according to a regime defined by Fillon et al. [28]. A cyclic heating and cooling procedure, already described elsewhere [19], was repeated by heating the sample at a temperature 3 °C lower than that of the previous annealing, until a heating temperature close to 40 °C was reached. Melting patterns of the samples thus prepared were recorded at a heating rate of 10 °C/min. The final heating scan after this thermal fractionation reveals a series of multiple melting peaks (as shown in Fig. 1) that are a reflection of the multiple mean lamellar thicknesses obtained.

2.4. Fourier transform infrared spectroscopy

All the materials were studied by means of FTIR spectroscopy. FTIR spectra were recorder in transmission mode with a 4 cm^{-1} resolution using a Nicolet 6700 spectrometer. The spectrum region analyzed was between 2000 and 1600 cm^{-1} where absorption bands associated with carbonyl groups appear which indicates the occurrence of oxidative degradation. For comparative proposes, a carbonyl index was defined as the ratio between the carbonyl band centered at 1720 cm^{-1} to a reference band centered at 2020 cm^{-1} corresponding to methylene stretching.

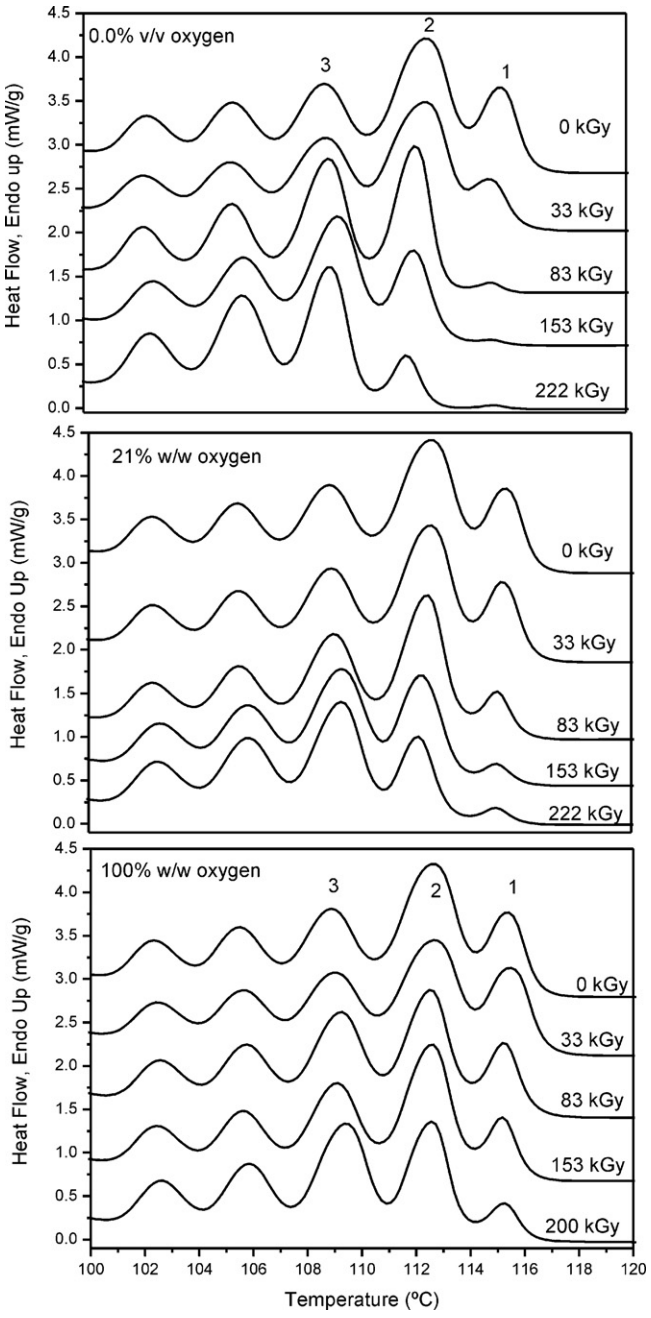

Fig. 1. SSA final endotherms for thin samples without antioxidant irradiated at three different oxygen concentrations.

3. Results and discussion

Table 1 shows standard DSC results for thin samples irradiated without antioxidant, to remark some details already known from

Table 1
Crystallinity (%) and melting temperature (°C) by thin, without antioxidant samples.

Dose (kGy)	0% v/v Oxygen		21% v/v Oxygen		100% v/v Oxygen	
	T_m (°C)	Crystallinity (%)	T_m (°C)	Crystallinity (%)	T_m (°C)	Crystallinity (%)
0	115.7 ± 0.2	34.9 ± 0.1	115.7 ± 0.2	34.9 ± 0.1	115.7 ± 0.2	34.9 ± 0.1
33	111.4 ± 0.3	34.2 ± 0.5	111.6 ± 0.3	34.7 ± 0.3	112.1 ± 0.2	35.1 ± 0.1
83	109.5 ± 0.4	33.2 ± 0.3	111.1 ± 0.1	33.9 ± 0.1	111.7 ± 0.3	34.5 ± 0.4
153	109.3 ± 0.2	32.8 ± 0.3	110.0 ± 0.4	33.8 ± 0.5	111.3 ± 0.1	34.4 ± 0.3
222	108.0 ± 0.1	31.8 ± 0.4	109.7 ± 0.2	32.4 ± 0.3	110.5 ± 0.2	33.8 ± 0.2

literature [5–7]. The presence of increasing oxygen concentrations accelerates its reaction with the free radicals formed by the irradiation process, reducing the chains crosslinking efficiency and thus favoring the chains scission processes. This point is qualitatively reflected in the changes of total crystallinity: smaller changes are found for samples irradiated under atmosphere richer in oxygen, as scission frees chains ends, while crosslinking reduces chains mobility needed for crystallization by introduction of topological restraints. Overall, crystallinity changes with radiation dose increase are not large, with a maximum of about 9% for highest radiation dose under nitrogen atmosphere; therefore all further analysis will be done disregarding any crystallinity changes. This is in accordance with reported by other authors who found no significant changes in the melting temperature and enthalpy of fusion after irradiation of polyethylene [29–31].

The formation of chain crosslink junctions affects the reorganization and chain folding during the crystallization process that result in a reduction in the crystallinity, and presumably cause the formation of crystals of smaller size and less perfect. Hence, the temperature and the heat of fusion decrease with dose due to an increment in the degree of chain crosslinking. Small reductions of the average crystallites thickness are reflected as temperature changes of the maximum of the fusion peak. This effect seems to be more closely related to chains crosslinking, as samples irradiated in nitrogen atmosphere show a more pronounced effect. As the SSA preparation process includes melting and recrystallization of the already irradiated and reacted samples, changes in the final melting endotherms (peak and position) reflect most details of molecular structural changes.

Fig. 1 shows SSA final melting endotherms for thin samples without antioxidant irradiated in atmospheres with three different oxygen concentrations. Antioxidant was removed to avoid competition with oxygen in reactions with free radicals, which may mask results [5,32]. Special attention is centered at the higher temperature melting peaks that correspond to thicker lamellae, as these reflect more faithfully details of the true distribution of crystallizable polymethylene sequences lengths in the liquid state. Lamellae grown at lower annealing temperatures are formed from chains that have more restricted diffusion and folding movements. We numbered peaks starting from the highest melting temperature placed at about 115 °C. For samples irradiated without oxygen, crosslinking quickly restricts mobility, and peaks 1 and 2 are reduced faster than for samples irradiated under oxygen-containing atmospheres. For samples irradiated under highest oxygen concentration, peak 1 shows a small increase for low radiation doses, due to faster chain scission for tertiary carbons in the main chain [18,19,24,25]. Therefore, changes in the areas under melting peaks 1 and 2 are the most sensitive and useful for analysis and modeling. Most noticeable effects are caused by reactions affecting the tertiary carbons linked to the longest crystallizable polymethylene sequences. Therefore, we here propose using data on peaks 1 and 2 to model early stages of combined scission-crosslinking processes. Simplest models will be advanced in future publications.

Comparative information can be directly extracted from Table 2. Only those temperatures capable of producing self nucleation and annealing (T_s) are reported in Table 2, since they are directly responsible for the annealed crystals that subsequently melt during the final heating run shown in Fig. 1. Melting area for peaks placed at lower temperatures are not considered, as they do not give much useful information for the purpose of this work. The column labeled as T_m includes only peak melting temperatures results for SSA final melting endotherms corresponding to non-irradiated samples, because these values may shift slowly as irradiation dose is increased. Area fractions changes indicate changes in the amount of uninterrupted crystallized polymethylene sequences of a particular length range. For instance, samples irradiated in nitrogen atmosphere with only 33 kGy present a reduction of 4% of the crystals mass that melt at about 115 °C. As total crystallinity is about 40%, we can safely conclude that reactions that affect to less than 1.7% of the polymer present can be clearly shown as changes of the partial area for peak 1. Even more, if we recall that the average lamellae thickness (6 nm) includes about 60 carbon atoms [19], then we estimate that reactions on 0.035% of total carbon atoms can be detected.

Table 2
Areas Fractions at applied dose in different atmospheres by thin samples without antioxidant.

Atmosphere	T_s (°C)	T_m (°C)	Partial area (%)				
Dose (kGy)			0	33	83	153	222
0% v/v Oxygen	117	115.3	10.6	6.2	0.8	0.3	0.2
	114	112.6	24.7	24.9	19.2	13.1	6.0
	111	108.9	15.8	18.1	22.6	23.9	21.8
	108	105.5	11.9	12.7	14.4	16.5	21.0
	105	102.2	10.2	10.5	12.2	13.6	15.2
21% v/v Oxygen	117	115.3	10.6	9.2	4.9	1.9	1.7
	114	112.6	24.7	23.9	23.2	16.8	12.3
	111	108.9	15.8	16.3	18.9	22.1	23.1
	108	105.5	11.9	12.2	13.1	15.7	17.3
	105	102.2	10.2	10.7	11.3	12.4	13.5
100% v/v Oxygen	117	115.3	10.6	12.7	8.9	7.0	4.2
	114	112.6	24.7	22.6	20.2	23.9	18.3
	111	108.9	15.8	16.1	18.5	18.4	21.8
	108	105.5	11.9	12.0	13.3	12.8	14.5
	105	102.2	10.2	9.9	10.6	10.8	12.0

Fig. 2a and b shows SSA results for low and medium irradiation dose values for thin samples without antioxidant. Fig. 2a shows results corresponding to samples irradiated with 33 kGy. Samples irradiated in nitrogen atmosphere show a reduction in the area under peak 1, due to crosslinking reactions. For samples irradiated under air or under oxygen, peak 1 is almost unchanged, because oxygen reacts faster with free radicals, inhibiting the crosslinking process to some extent. Peak 2 area is slightly more reduced in oxygen atmosphere, probably because of chains scission (free radicals inhibition). We can conclude that peak 1 area changes little because of a fortunate compensation between chains scission and crosslinking for this irradiation dose.

Fig. 2b corresponds to 83 kGy. We observe distinct differences for samples irradiated under atmospheres with different oxygen concentrations. Peak 1 decreases with decreasing oxygen content, because scission of tertiary carbon atoms is then reduced. As mentioned above, Peak 1 is considered as the most sensitive to tertiary carbons scission, because this scission frees a considerable chain length that may then be incorporated to the thicker lamellae at the annealing process [18]. Thicker lamellae, formed at the highest annealing temperature, will reflect small changes in molecular structure.

As Fig. 2 shows only part of the melting enthalpy, visual observation may be misleading. For modeling purposes we refer to partial areas shown in Table 2, always keeping in mind the fact that total melting enthalpy remains essentially constant. For 33 kGy the peak 1 area fraction increases with oxygen concentration, from 6.2% to 9.2% and to 12.7%, due to chains scission. For 83 kGy the peak 1 area fraction is changed from 10.6% for the non-irradiated samples to 0.8% for samples irradiated under nitrogen, to 4.9% under air, and to 8.9% under oxygen.

So far, we have been focusing the analysis on samples irradiated at low doses. The reason is because at larger reaction extents the crosslinking and scission reactions will compete, making the final molecular structure more complex and less useful for modeling

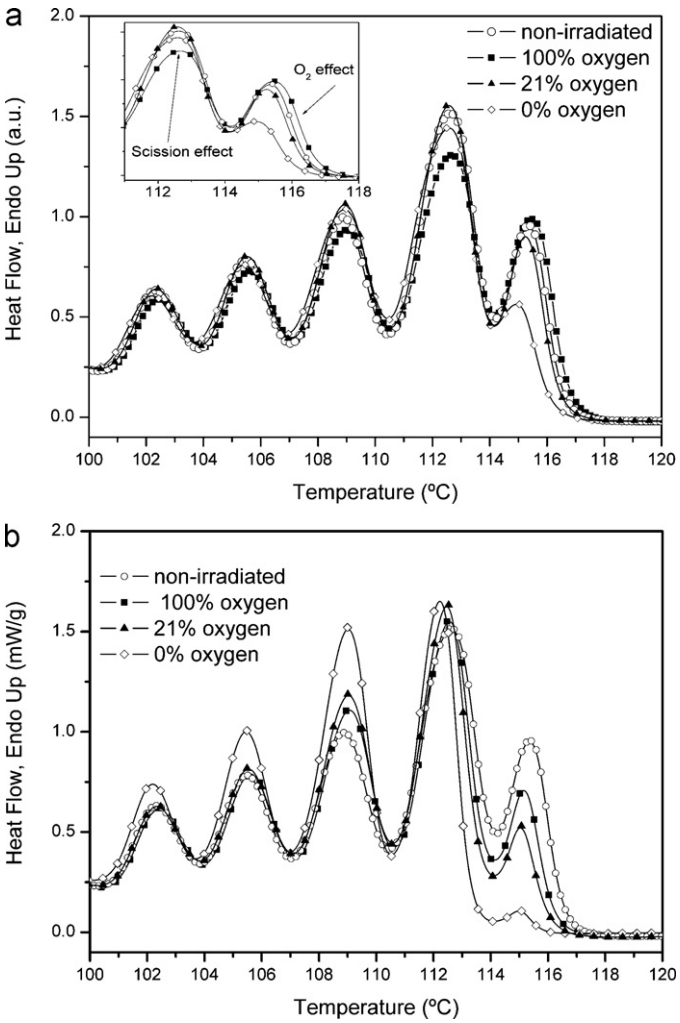

Fig. 2. SSA final endotherms for thin samples without antioxidant irradiated at (a) 33 and (b) 83 kGy in three different oxygen concentrations.

purposes. Changes for samples irradiated with 153 and 222 kGy are more evident, as shown in Table 2.

Other factors must be considered while collecting data for modeling purposes. When gases in the atmosphere surrounding the sample participate in the whole reaction, as for instance oxygen, the gas concentration and the sample thickness will play different roles A small amount of oxygen will be dissolved in the sample before irradiation time, and quickly react first with the free radicals formed due to the irradiation energy. In addition, un-reacted free radicals homogeneously distributed inside the crystals structure could slowly react with oxygen when the samples were exposed

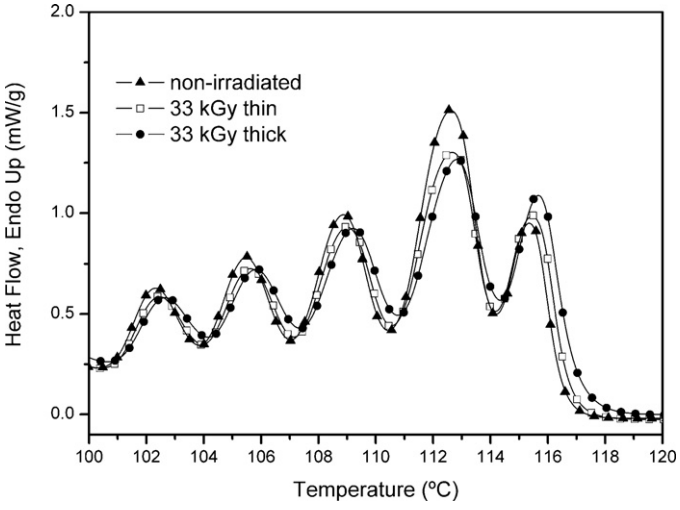

Fig. 3. SSA final endotherms for samples thick and thin without antioxidant irradiated at 33 kGy in 100% oxygen atmosphere.

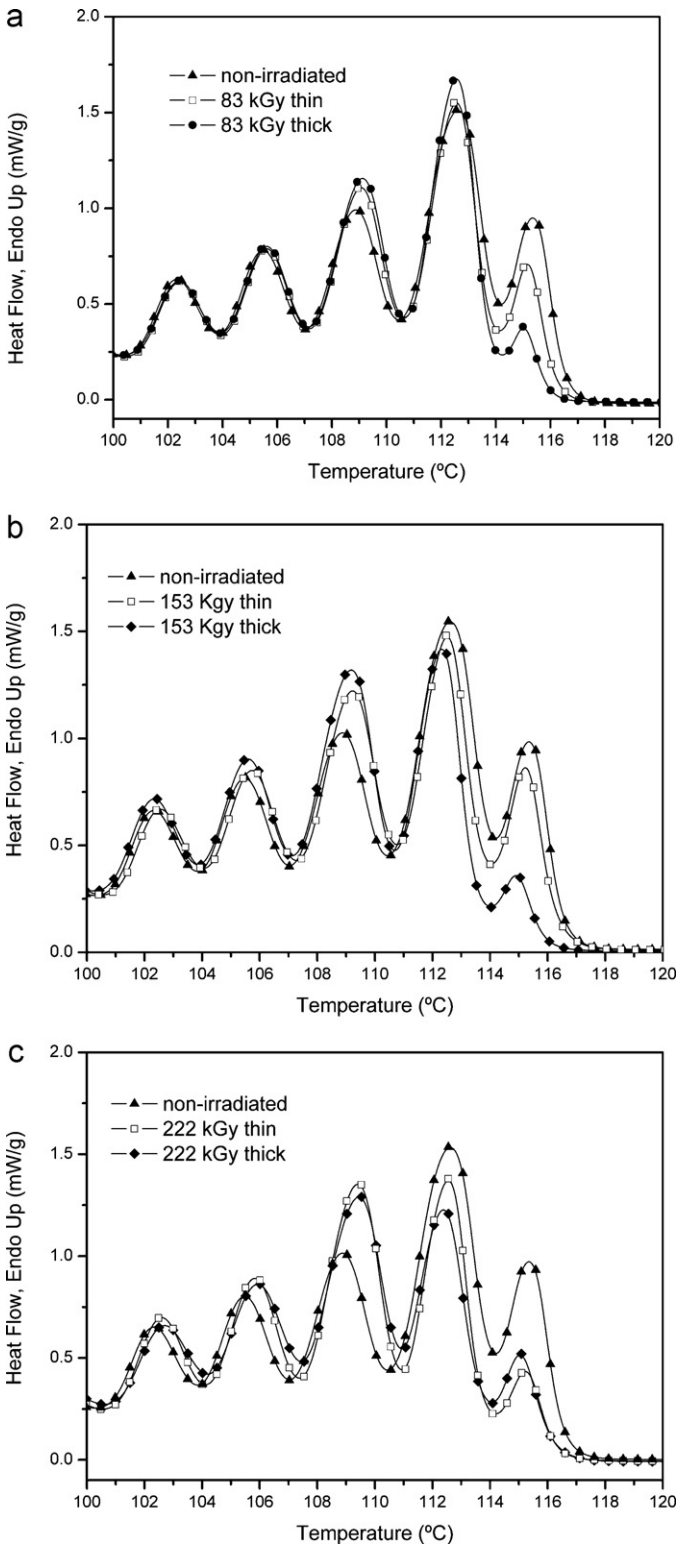

Fig. 4. SSA final endotherms for samples thick and thin without antioxidant irradiated at (a) 83 kGy, (b) 153 kGy and (c) 222 kGy in 100% oxygen atmosphere.

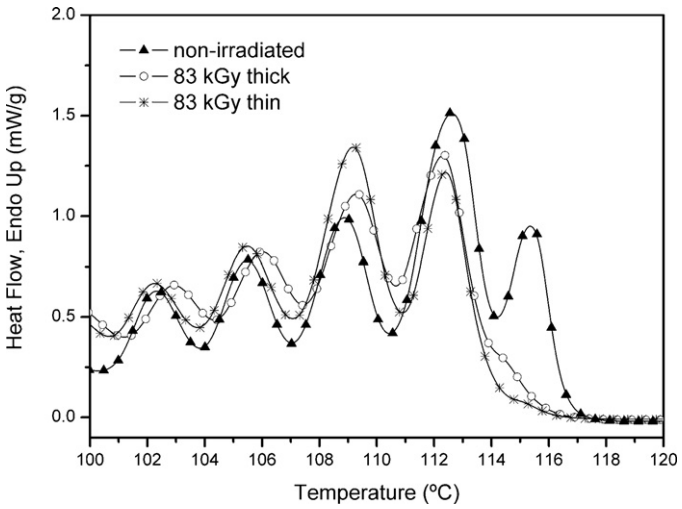

Fig. 5. SSA final endotherms for samples thick and thin without antioxidant irradiated at 83 kGy, in 0% oxygen atmosphere.

to the air atmosphere. For this reaction extent we ought not to expect any influence of the sample thickness on the final polymer structural changes. Fig. 3 shows that samples labeled as "thin" and "thick", do not show any noticeable difference when irradiated with only 33 kGy. For larger irradiation doses, if the concentration of the oxygen initially dissolved is depleted enough by fast chemical reactions, then a quite slower diffusion process will allow the oxygen present in the atmosphere to reach the free radicals just formed inside the polymer sample. As we progress in depth (or diffusion distance) we find less oxygen available for scission reactions, and the slow diffusion process will cause differences in observable molecular changes inside the samples. At the sample surface, the almost constant oxygen concentration values will favor chain scission reactions. Deeper in the sample, lower oxygen concentration will favor crosslinking reactions. It has already been observed that when polyethylene is exposed to irradiation in air, heterogeneous materials form; that is, the resulting molecular structure changes from the skin to the core, as a consequence of an oxidation process controlled by oxygen diffusion [33,34]. Therefore we must expect some influence of the samples thickness on the final molecular structure.

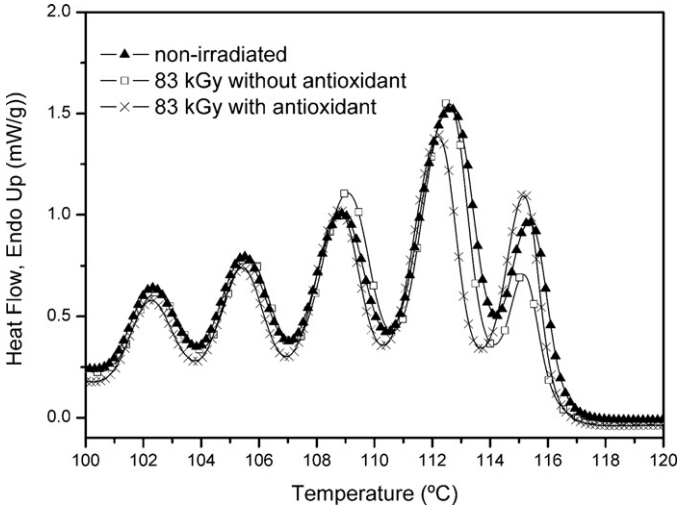

Fig. 6. SSA final endotherms for samples with and without antioxidant irradiated at 83 kGy in 100% oxygen atmosphere.

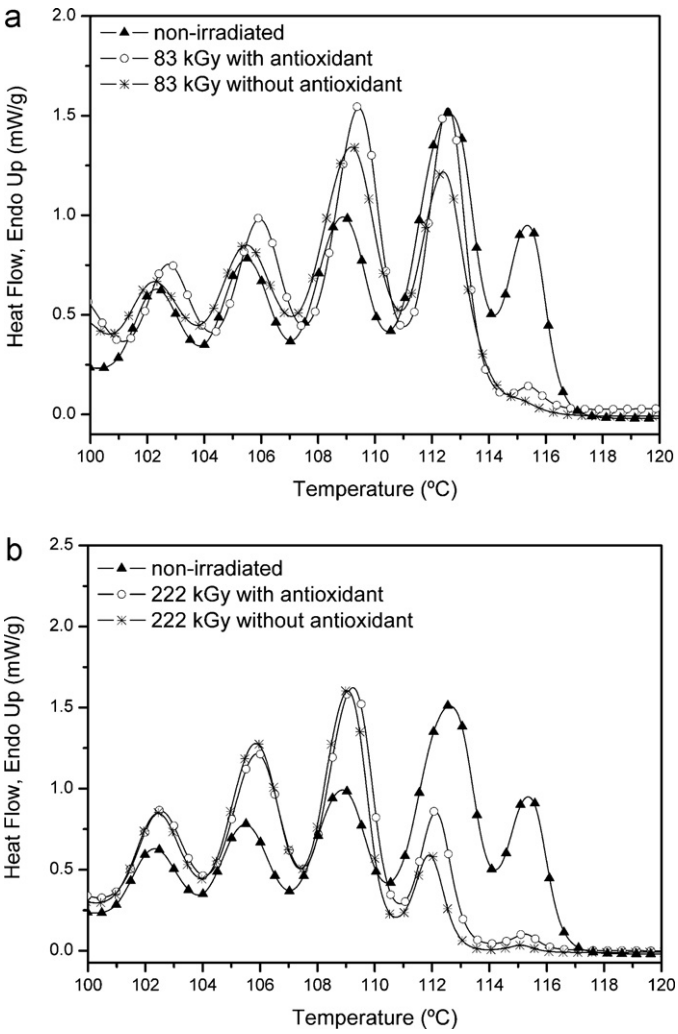

Fig. 7. SSA final endotherms for samples with and without antioxidant irradiated at (a) 83 kGy (b) 222 kGy in 0% oxygen atmosphere.

Fig. 4a and b shows the expected effect of sample thickness described above. Here we feel we must make clear that SSA results show an average result for the sample thickness, as full disks were cut through the samples and placed in the DSC pan. Fig. 4c does not show any appreciable influence of samples thickness, here because for this large dose value the changes in molecular structure include enough crosslinking to mask the effect of chains scission on the peak 1 evolution. To further analyze the effects of oxygen diffusion into the samples, overall analysis may benefit from spectroscopic techniques, like FTRaman, that may use smaller samples mass and be able to find differences in reactions products concentrations between surface and bulk.

The effect of sample thickness, as influenced strongly by the oxygen diffusion rate, will depend at least on samples crystallinity and on irradiation rates and temperatures. The proper size for any sample to be considered thin or thick must be tested for each polymer type, for each irradiation dose rate and for each irradiation temperature. Preliminary results have been published for very low oxidation reaction rates, conducted at temperatures that promote oxygen diffusion [24].

As nitrogen does not have any influence on the crosslinking vs. chain scission reactions competition, we do not expect the samples thickness to have any effect on the final polymer molecular structure, as shown in Fig. 5. The same type of behavior is observed for any of the irradiation dose values used for this work.

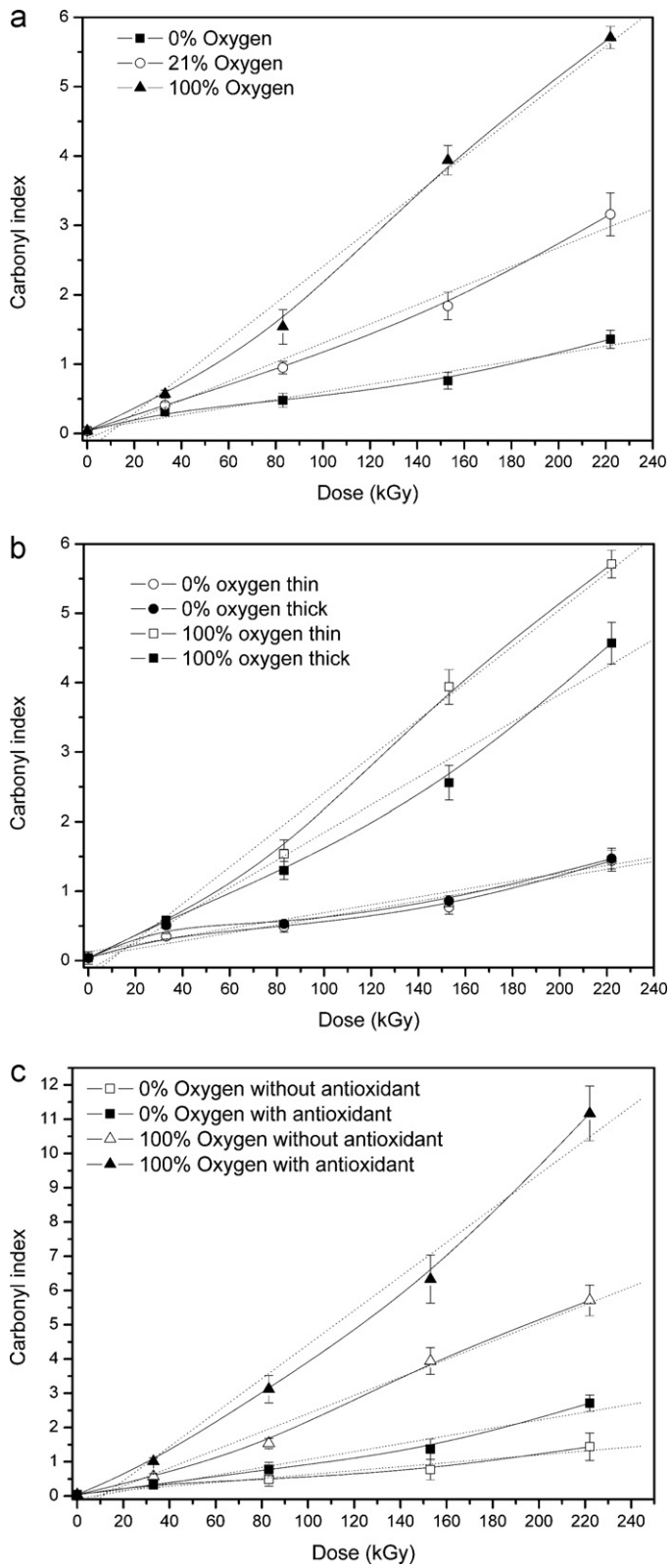

Fig. 8. Carbonyl index as a function of dose. (a) Thin samples without antioxidant irradiated in three different oxygen concentrations. (b) Thin and thick samples without antioxidant irradiated in 0 and 100% oxygen concentrations. (c) Thin samples with and without antioxidant irradiated in 0 and 100% oxygen concentrations.

Usual components of polyolefins formulations include antioxidants that are at first designed to quickly react with oxygen free radicals that may be present in hot air in contact with polymer melt been processed. In this context, we expect antioxidants to behave in a similar way as oxygen previously dissolved in the polymer. Free radicals formed on the chains carbons by irradiation energy will also react quickly with antioxidants, favoring chains scission in the same way as oxygen does, and its effect will not be dependent on samples thickness and end at some irradiation dose value. Therefore we expect the antioxidant effect to extend the irradiation dose level for which the final molecular structure does not depend on samples thickness. Fig. 6 shows the effect of antioxidant for samples irradiated in oxygen atmosphere, which clearly promotes more chains scission than oxygen alone.

Small but recognizable differences can be found for samples irradiated under nitrogen atmosphere with and without antioxidant. Fig. 7a and b shows different evolutions of peaks 1 and 2. Antioxidant retards the reduction of areas under these peaks for irradiation doses of 83 and 222 kGy.

We qualitatively compare the samples in terms of bulk oxidation level by defining a carbonyl index as described in Section 2. Here the word bulk implies that the carbonyl groups may be located at the polymer chains or at the antioxidant reaction products. Fig. 8 shows measured carbonyl index values as functions of irradiation dose. As the FTIR measurements are done in the transmittance mode for uncut samples, the reported carbonyl index values reflect average values. When analyzing these results we must consider that the partition of carbonyl species (polymer vs. antioxidant) might be affected by the activity of the antioxidant, as well as by a small amount of dissolved oxygen that might have remained in the initial samples. The results reported in Fig. 8a, show that the carbonyl index increases steadily with the irradiation dose value for thin samples without antioxidant. These samples are shown first because there is no influence of thickness or antioxidant concentration. As expected, oxygen concentration increases raise the level of the carbonyl index [35–37].

Fig. 8b shows the effect of samples thickness in atmospheres with and without oxygen. Thick samples irradiated in oxygen show a lower carbonyl index than thin samples. Samples irradiated in nitrogen atmosphere show no difference. Both bulk measurements – SSA and FTIR – show coincident qualitative results.

Fig. 8c shows that both, polymer and antioxidant, give carbonyl groups as final reaction products. For samples irradiated in nitrogen atmosphere, most probably a small amount of oxygen remains dissolved in the samples throughout the whole process, resulting in a small carbonyl groups concentration. In addition, a contribution to the carbonyl concentration build up may come from the reaction of free radicals – which are trapped in the structure – with oxygen in the air when the samples are exposed to the atmosphere. The presence of oxygen in the irradiation atmosphere gives higher reaction rates.

For all samples, an almost linear fit is obtained, as shown in dotted lines. In good agreement with results shown in the literature.

This set of carbonyl index results suggests that both techniques – SSA and FTIR, combined with spectroscopic techniques that may measure carbonyl concentrations at the polymer surface – ought to be used in a complementary way to explore the influence of antioxidant on the reactions conducted on the polymers chains.

4. Conclusions

The SSA technique results analysis, focused mainly on the evolution of the higher temperature melting peaks, gives information on the changes of longer polymethylene crystallizable lengths. LDPE is specially suited for this type of studies, as its molecular

structure contains both, short and long branches. The scission reactions of the tertiary carbon atoms produce very different consequences on the SSA results, depending of whether a short or a long branch is attached there. Easily recognizable differences can be found for samples irradiated in atmospheres with different oxygen concentrations, with and without antioxidant. Also the effects of samples thickness are demonstrated.

Acknowledgements

The authors acknowledged to the National Research Council of Argentina (CONICET) and ANPCyT (PICT07-1906) for the financial support.

References

[1] M. Gahleitner, Melt rheology of polyolefins, Prog. Polym. Sci. 26 (2001) 895–944.
[2] R.L. Clough, High energy radiation and polymers: a review of commercial processes and emerging applications, Nucl. Instrum. Methods B 185 (2001) 8–33.
[3] A.B. Lugao, H. Otaguro, D.F. Parra, A. Yoshiga, L.F.C.P. Lima, B.W.H. Artel, S. Liberman, Review on the production process and uses of controlled rheology polypropylene-Gamma radiation versus electron beam processing, Radiat. Phys. Chem. 76 (2007) 1688–1690.
[4] A. Singh, Irradiation of polyethylene: some aspects of crosslinking and oxidative degradation, Radiat. Phys. Chem. 56 (1999) 375–380.
[5] M. Ghaffari, V. Ahmadian, Investigation of antioxidant and electron beam radiation effects on the thermal oxidation stability of low-density polyethylene, Radiat. Phys. Chem. 76 (2007) 1666–1670.
[6] J.C.M. Suarez, E.E.C. Monteiro, E.B. Mano, Study of the effect of gamma irradiation on polyolefins-low density polyethylene, Radiat. Phys. Chem. 75 (2002) 143–151.
[7] I. Badr, Z. Ali, A. Zahran, R.M. Khafagy, Characterization of gamma irradiated polyethylene films by DSC and X-Ray diffraction techniques, Polym. Int. 49 (2000) 1555–1560.
[8] N. Andreucetti, L.L. Lagos, O. Curzio, C. Sarmoria, E.M. Vallés, Model linear ethylene-butene copolymers irradiated with γ-rays, Polymer 40 (1999) 3443–3450.
[9] C.J. Perez, E.M. Vallés, M.D. Failla, Modification of model ethylene-butene copolymers using an organic peroxide, Polymer 46 (2005) 725–732.
[10] J. Borrajo, C. Cordon, J.M. Carella, S. Toso, G. Goizueta, Modeling the fractionation process in TREF systems: thermodynamic simple approach, J. Polym. Sci. B: Polym. Phys. 33 (1995) 1627–1632.
[11] J.B.P. Soares, B. Monrabal, J. Nieto, J. Blanco, Crystallization analysis fractionation (CRYSTAF) of poly(ethylene-1-octene) made with single-site type catalysts: a mathematical model for the dependence of composition distribution on molecular weight, Macromol. Chem. Phys. 199 (1998) 1917–1923.
[12] G. Elicabe, J.M. Carella, J. Borrajo, Modeling the fractionation process in TREF systems. 2. Numerical-analysis, J. Polym. Sci. B: Polym. Phys. 34 (1996) 527–533.
[13] J.P. Tomba, J.M. Carella, J.M. Pastor, Fractionation process in TREF systems: validation of thermodynamic model and calculation procedure by Raman LAM studies, J. Polym. Sci. Part B: Polym. Phys. 43 (2005) 3083–3092.
[14] E. Adisson, M. Ribeiro, A. Deffieux, M. Fontanille, Evaluation of the heterogeneity in linear low density polyethylene comonomer unit distribution by differential scanning calorimetry: characterization of thermally treated samples, Polymer 33 (1992) 4337–4342.
[15] A.J. Müller, Z.H. Hernandez, M.L. Arnal, J.J. Sanchez, Succesive self-nucleation/annealing (SSA): a novel technique to study molecular segregation during crystallization, Polym. Bull. 39 (1997) 465–472.
[16] L. Marquez, I. Rivero, A.J. Müller, Application of the SSA calorimetric technique to characterize LLDPE grafted with diethyl maleate, Macromol. Chem. Phys. 200 (1999) 330–337.
[17] A.J. Müller, M.L. Arnal, Thermal fractionation of polymers, Prog. Polym. Sci. 30 (2005) 559–603.
[18] C.J. Pérez, J.M. Carella, Early detection of degradation in a semi-crystalline polyolefin by a successive self-nucleation and annealing technique, Polym. Degrad. Stab. 92 (2007) 1213–1218.
[19] C.J. Pérez, N. Villarreal, J.M. Pastor, M.D. Failla, E.M. Vallés, J.M. Carella, The use of SSA fractionation to detect changes in the molecular structure of model ethylene-butene copolymers modified by peroxide attack, Polym. Degrad. Stab. 94 (2009) 1639–1645.
[20] C. Baker, L. Mandelkern, The crystallization and melting of copolymers I: the effect of the crystallization temperature upon the apparent melting temperature of polymethylene copolymers, Polymer 7 (1966) 7–21.
[21] O. Darrás, R. Seguela, Surface free energy of the chain-folding crystal faces of ethylene-butene random copolymers, Polymer 34 (1993) 2946.
[22] A. Lorenzo, M.L. Arnal, A.J. Müller, M.C. Lin, H.L. Chen, SAXS/DSC analysis of the lamellar thickness distribution on a SSA thermally fractionated model polyethylene, Macromol. Chem. Phys. 212 (2011) 2009–2016.
[23] A. Muller, A. Lorenzo, M. Arnal, Recent advances and applications of successive self-nucleation and annealing (SSA) high speed thermal fractionation, Macromol. Symp. 277 (2009) 207–214.
[24] C. Sarmoria, C.J. Pérez, M.D. Failla, J.M. Carella, E.M. Vallés, Efecto de la degradación termo-oxidativa en la MWD de segmentos cristalizables en polietilenos, in: IX Simposio Argentino de Polímeros, Bahía Blanca, Argentina, Noviembre 2011, 2011.
[25] C. Sarmoria, PLAPIQUI-CONICET, Universidad Nacional del Sur, Bahía Blanca, Argentina, Personal communication.
[26] Y. Paolini, G. Ronca, J. Feijoo, E. Da Silva, J. Ramirez, A. Muller, Application of the SSA calorimetric technique to characterize an XLPE insulator aged under multiple stresses, Macromol. Chem. Phys. 202 (2001) 1539–1547.
[27] J.M. Carella, J.T. Gotro, W.W. Graessley, Thermorheological effects of long chain branching in entangled polymer melts, Macromolecules 19 (1986) 659–665.
[28] B. Fillon, A. Thierry, J. Wittmann, B. Lotz, A. Thierry, Self-nucleation and enhanced nucleation of polymers. Definition of a convenient calorimetric efficiency scale and evaluation of nucleation additives in isotactic polypropylene (α phase), J. Polym. Sci. B: Polym. Phys. 31 (1993) 1383–1393.
[29] F.J. Zoepfel, V. Markovic, J. Silverman, Differential scanning calorimetry studies of irradiated polyethylene: I. Melting temperatures and fusion endotherms, J. Polym. Sci. A: Polym. Chem. 22 (1984) 2017–2032.
[30] H.A. Khonakdar, S.H. Jafari, U. Wagenknecht, D. Jehnichen, Effect of electron-irradiation on cross-link density and crystalline structure of low- and high-density polyethylene, Radiat. Phys. Chem. 75 (2006) 78–86.
[31] C.J. Pérez, E.M. Vallés, M.D. Failla, The effect of post-irradiation annealing on the crosslinking induced by gamma-irradiation of high density polyethylene, Radiat. Phys. Chem. 79 (2010) 717–724.
[32] L.J. Novakovic, O. Gal, Irradiation effect on polyethylene in the presence of an antioxidant and trifunctional monomers, Polym. Degrad. Stab. 50 (1995) 53–58.
[33] L. Audouin-Jirackova, G. Papet, J. Verdu, Effect of radiochemical ageing on the tensile properties of high density polyethylene, Eur. Polym. J. 25 (1989) 181–186.
[34] L. Audouin-Jirackova, G. Papet, J. Verdu, Diffusion controlled radiochemical oxidation of low density polyethylene–II kinetic modeling, Int. J. Radiat. Appl. Instrum. C: Radiat. Phys. Chem. 33 (1989) 329–335.
[35] E. Suljovrujic, Z. Kacarevic-Popovic, D. Kostoski, J. Dojcilovic, Effect of ageing on the dielectric relaxation of oriented and gamma irradiated LDPE, Polym. Degrad. Stab. 71 (2001) 367–373.
[36] D. Kostoski, J. Dojcilovic, E. Suljovrujic, L. Novakovic, Effects of charge trapping in gamma irradiated and accelerated aged low-density polyethylene, Polym. Degrad. Stab. 91 (2006) 2229–2232.
[37] E. Suljovrujic, D. Kostoski, J. Dojcilovic, Charge trapping in gamma irradiated low-density polyethylene, Polym. Degrad. Stab. 74 (2001) 167–170.